Concealing Messages at the Atomic-Thin Level by Reaching the Limit of Writing

Chao Hou, Qirong Yang, Jianxin Guan, Jingwen Deng, Zihan Xu, Zhihao Yu,* and Junrong Zheng*

The evolution of writing system reflects the development of civilization. Using a single molecular layer of "ink" to record invisible messages on an atomic-layered paper represents the ultimate thinness of classical writing system and steganography. A stable and convenient atomic-thin information steganography under ambient conditions is realized using a monolayer of water as "ink," an atomic layer of MoS₂ as paper, and a laser as the pen. Physically adsorbed monolayered water molecules produce p-type doping to the monolayer MoS₂, leading to its photoluminescence (PL) enhancement. Information is written using a laser to remove surface water with designed patterns and is read out by PL imaging. The information is transparent to visible light and can retain for at least one week until erased by a humidification treatment. The method reaches the thinnest limit of writing and achieves repeatable data storage, providing promising applications in steganography and high-density storage at the atomic-thin level.

1. Introduction

From prehistoric symbolic murals carved on caves by stone, to the confidential information written on letter paper by invisible ink, the continuous improvement of writing system has witnessed human progresses. A special type of writing, steganography, which is usually taken as a top secret, is evolving with time. The formulas of secret ink used in the First World War were ordered to remain hidden from the public in 2002,[1] even though these secret writing methods merely stay at the primary level of chromogenic reaction. At the turn of this century, it was

C. Hou, Q.-R. Yang, J.-X. Guan, J.-W. Deng, Z.-H. Yu, J.-R. Zheng
College of Chemistry and Molecular Engineering
Beijing National Laboratory for Molecular Sciences
Peking University
Beijing 100871, China
E-mail: zhihaoyu@pku.edu.cn; junrong@pku.edu.cn
Z.-H. Xu
Shenzhen Sixcarbon Technology
Shenzhen 518106, China

The ORCID identification number(s) for the author(s) of this article can be found under https://doi.org/10.1002/admt.202101089.

reported that the steganographic technique could be advanced to the molecular level by concealing secret messages in DNA-based microdot[2,3] and macromolecules.[4] Ultrathin and large-area semiconductive polymers can also be fabricated for miniaturized energy storage devices through an interfacial method and laser scribing.[5–7] By thinning down paper and ink to the atomic scale, one may reach the limit of writing system and take steganography a step further, even enabling the storage of data in an atomic-thin memory. The path to store information at the atomic limit can be carried out by scanning probe microscopes (SPMs), e.g., scanning tunneling microscope (STM) through directly manipulating lattice locations,[8,9] charge state[10,11] or magnetization states,[12–14] or atomic force microscope (AFM) methods like dip-pen nanolithography (DPN)[15,16] that can deliver a wide range of substances onto various substrates.[16–18] The SPM methods require low temperature, clean surface, ultra-high vacuum environment, and/or complicated operations,[19,20] and their information readout typically relies on delicate SPM or electronic microscopes. These are undesirable features for steganography of which users are usually under intense pressure with limited conditions and have limited time to work.

Herein, using a monolayer of water as "ink," an atomic layer of MoS₂ as paper, and a laser as pen, concealing information at the atomic-thin level is achieved under ambient conditions in a rewritable manner.

2. Results and Discussion

An optical image of the as-grown MoS₂ monolayer is displayed in **Figure 1**a. Its photoluminescence (PL) signal is enhanced upon water adsorption (from black to blue curve), and the desorption of water by laser irradiation (from blue to red curve) suppresses the PL enhancement (Figure 1b). By the way, the PL changes with the environmental relative humidity (RH) are shown in Figure S1 in the Supporting Information. The PL intensity changes little when RH is less than 70%, but increases rapidly when RH is more than 70%. There is a process for adsorption to reach equilibrium, and only enough adsorption can enhance the PL significantly. Raman spectroscopic

**ADVANCED
SCIENCE NEWS**

www.advancedsciencenews.com

**ADVANCED
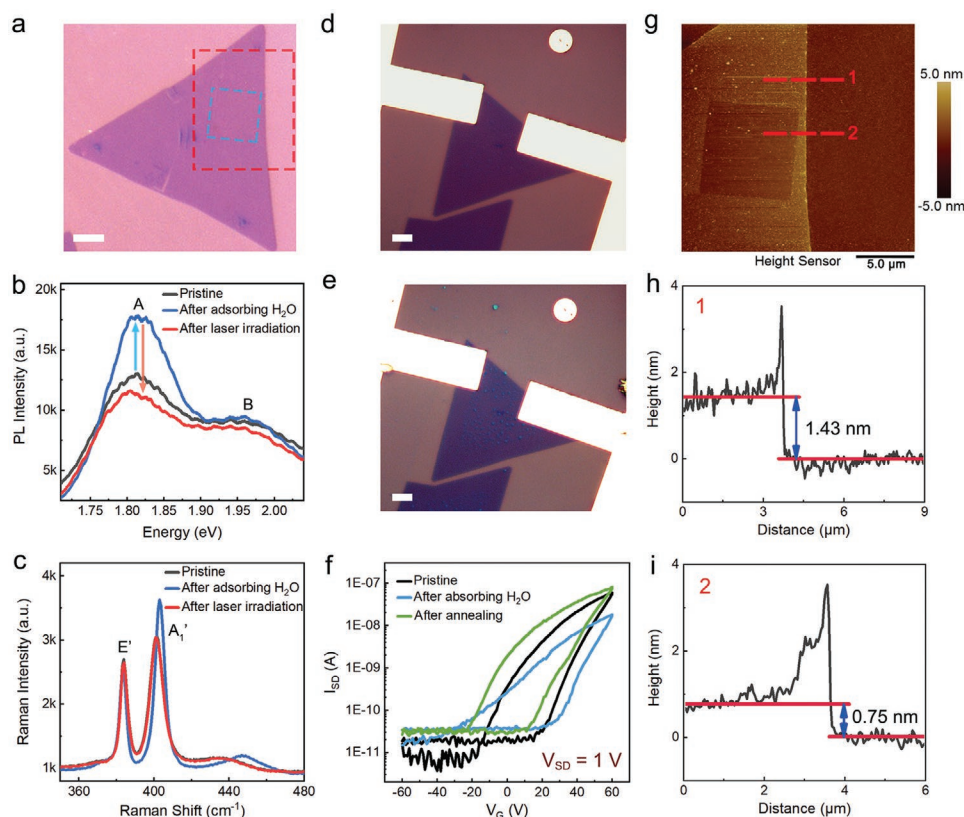MATERIALS
TECHNOLOGIES**

www.advmattechnol.de

Figure 1. a) Optical image of a monolayered MoS_2 triangle domain. b) The PL and c) Raman spectra of the MoS_2 monolayer before and after corresponding treatments. Optical images of the monolayered MoS_2 FET device d) before and e) after adsorbing H_2O molecules. f) Source–drain current (I_{SD}) versus back gate voltage (V_G) curves with a source–drain voltage (V_{SD}) of 1 V for the FET device before and after corresponding treatments. g) AFM image for the red rectangle area in panel (a), including the laser-treated region denoted with blue rectangle. h,i) A line profile showing the height along the red line #1 and #2 in panel (g). Scale bars are all 5 µm.

measurements ÷ that the laser irradiation does little damage to the MoS_2 monolayer. As displayed in Figure 1c, adsorbing H_2O molecules blueshifts and intensifies the out-of-plane vibrational mode A_1' of MoS_2, whereas the in-plane vibrational mode E' stays unchanged (blue curve). After the laser irradiation treatment, the Raman spectrum (red curve) changes back to be almost identical to the pristine one (black curve), suggesting that there is little structural change within the monolayer of MoS_2. To investigate the mechanism of PL enhancement by adsorbing H_2O molecules, a field-effect transistor (FET) device is fabricated to explore the variations in carrier concentration of MoS_2. Figure 1d,e displays the optical images of the FET device before and after adsorbing H_2O molecules, respectively. Their appearances show no obvious change, but their electronic properties vary significantly. The source–drain current (I_{SD}) versus back gate voltage (V_G) curves in Figure 1f indicate that the pristine device (black curve) shows an n-type characteristic. After adsorbing H_2O molecules on the surface, the electron concentration drops sharply (blue curve), suggesting that the physically adsorbed H_2O molecules have a p-type doping effect to MoS_2. A p-type doping favors the formation and recombination of neutral excitons over negative trions. According to literatures,[21–23] neutral excitons have a faster radiative recombination rate than the negative trions and thus have a higher PL efficiency, leading to the PL enhancement. Once the adsorbed H_2O molecules are

erased by annealing in vacuum (200 °C for 3 h), the n-type characteristic (green curve) is restored, and in fact is even slightly enhanced compared to the pristine sample, because fewer water molecules are on the annealed sample.

The laser irradiation removing the surface H_2O molecules is further verified with AFM mapping. A square region by laser irradiation on the MoS_2 sample (the blue rectangle area denoted in Figure 1a) is not distinguishable by optical microscope, whereas it is clearly visible under AFM mapping (Figure 1g). The line profile in Figure 1h indicates that the thickness of the monolayer MoS_2 before laser treatment is 1.43 nm, which is higher than the theoretical value of monolayered MoS_2 owing to the adsorbed water. The average thickness of the laser-treated square region (Figure 1i) is measured to be 0.75 nm, consistent with the reported monolayer thickness of MoS_2.[24] The thickness reduction caused by laser treatment is about 0.68 nm, which agrees well with the thickness of a single layer of water molecules ($\approx$0.4 nm) plus the adsorption equilibrium distance ($\approx$0.2 nm).[25] The measured thickness of MoS_2 monolayer with adsorbed water is consistent with previous theoretical studies.[26,27]

By removing surface water in designed patterns with lasers and the readdition of water by humidification, rewritable data-encoding, and readout through simple PL mapping can be achieved. The encoding scheme is illustrated in **Figure 2**a. The sample is moisturized before laser writing, and then patterns
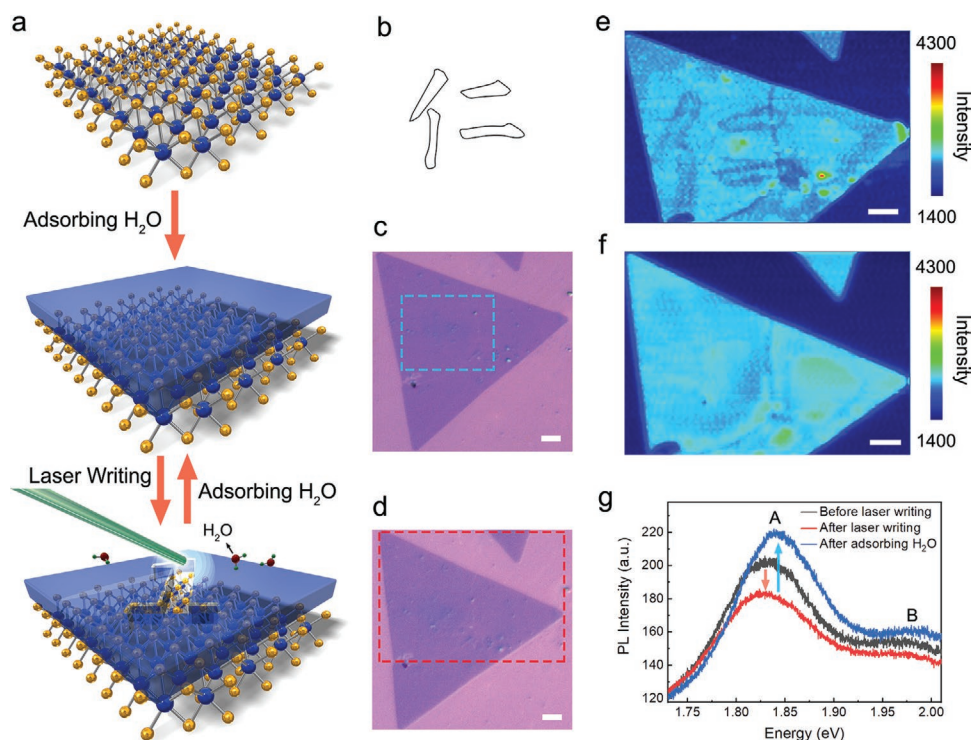
Figure 2. a) A scheme of laser writing and erasing cycle. b) A Chinese character meaning "benevolence" used as a laser irradiation pattern. c) Optical image of a MoS$_2$ monolayer triangle domain after laser writing "仁" inside the blue rectangle. d) Optical image of panel (c) after erasing the pattern by adsorbing H$_2$O molecules. The red rectangle denotes the area being mapped. e,f) PL mapping images (at 1.82–2.00 eV) corresponding to panels (c) and (d), respectively. g) PL spectra of the sample before (black curve) and after laser writing (red curve), and after erasing treatment (blue curve), respectively. Scale bars are all 4 μm.

are written directly onto the MoS$_2$ monolayer with a laser by removing the surface water. A home-built laser writing system is used to conduct the information-writing process (Figure S2, Supporting Information). The laser-written information is read out by PL imaging, and is erased by exposing the sample to a humid environment. Figure 2b displays a Chinese character "仁" with the meaning of benevolence that is written onto the MoS$_2$ monolayer. The writing of "仁" (Figure 2c) and the erasing of it with water adsorption (Figure 2d) do not produce observable changes on the sample's optical images. Through PL mapping, the written pattern is clearly visible (Figure 2e). Under ambient conditions (humidity < 30%), the written pattern can last for at least one week. The pattern is successfully erased after the sample is placed in a humid environment (relative humidity ≈85% for about 10 min) (Figure 2f). The PL spectra of the sample before any treatments (black curve), after laser writing (red curve), and after pattern-erasing by adsorbing H$_2$O molecules (blue curve) are displayed in Figure 2g. They are very similar to those in Figure 1b, of which the PL intensity is dependent on the surface water content as discussed above. During writing, the laser power density is carefully controlled at about 3.0×10^5 W cm^{-2} to ensure that the thermal energy generated by MoS$_2$ photoadsorption is sufficient for the removal of water but below the MoS$_2$ damage threshold. Overwriting with too much laser power can cause permanent damages to the MoS$_2$ monolayer and the written pattern cannot be erased by adsorbing H$_2$O molecules (Figure S3, Supporting Information).

The MoS$_2$ monolayer is rewritable for many times. **Figure 3** displays the PL images of "仁" written in the solid-filled form (upper panels) and erased (bottom panels) at the 1st, 10th, 20th, and 50th cycle. The upper panels are taken after each writing. "仁" is still visible after 50 writing/erasing cycles. The PL images in the bottom panels are taken after each humidification treatment, showing that "仁" is completely removed by the erasing process. To test how long the written pattern can last, we keep the sample in a container at 30% RH for a week right after the 20th writing. Water in the air has not been able to erase the written pattern for such a long period of time, and "仁" is still clearly distinguishable, as shown in the upper 20th panel in Figure 3. The corresponding optical images of the sample after each writing/erasing cycle also show no noticeable changes on the MoS$_2$ monolayer during the processes (Figure S4, Supporting Information).

Not only can a simple word or symbol be written with the method, but also a sentence and even a painting. The phrase "Nothing is Impossible" (**Figure 4**a–c) and the famous painting Mona Lisa (Figure 4d–f) are successfully written on continuous MoS$_2$ monolayered films. The line drawing of Mona Lisa (Figure 4f) is probably the thinnest portrait by far, since the "paper" is a monolayer of MoS$_2$ and the "pigment" is one layer of H$_2$O molecules.

The writing/erasing process is reasonably fast, dependent on the complexity of the written pattern. A more complexed pattern takes a longer time. With the same condition, writing "仁" and "π" of a similar size takes about 60 and 15 s, respectively. It takes less than 10 min to obtain their PL images by mapping. The erasing can be extremely fast. In a destructive way, if the sample is dipped into water or blown by breath, the pattern
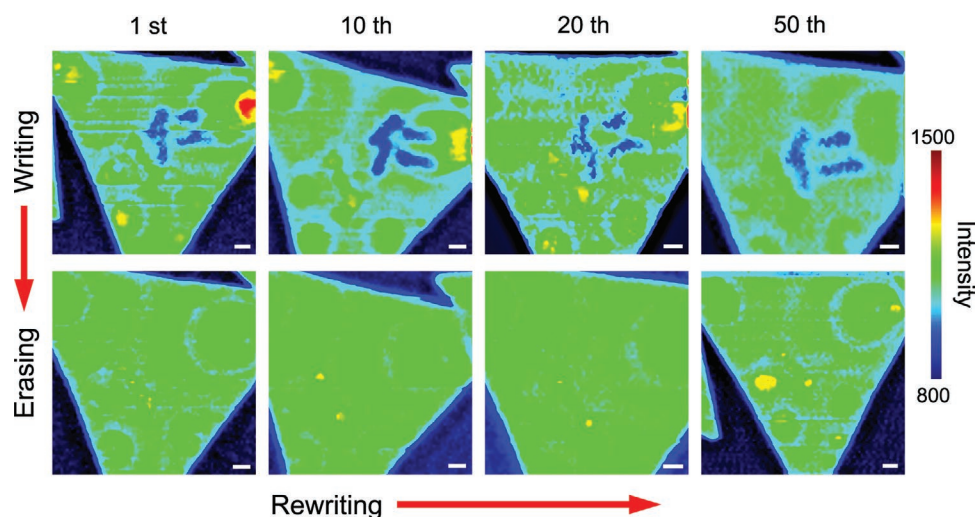
ADVANCED
SCIENCE NEWS
www.advancedsciencenews.com

ADVANCED
MATERIALS
TECHNOLOGIES
www.advmattechnol.de

Figure 3. The PL mapping for the 1st, 10th, 20th, and 50th laser writing (upper panels) and erasing (bottom panels) "⌐" on the same MoS$_2$ monolayer triangle domain. Scale bars are all 2 µm.

disappears immediately, but in most of our tries the MoS$_2$ monolayer is broken after the erasing process. In a nondestructive manner, the sample is placed in an environment with an RH of 85%, the written pattern disappears within 10 min. In total, it takes minutes for the entire writing/erasing/readout process. The time can be significantly shortened by optimizing the operation conditions and tools, e.g., using 2D PL imaging rather than point mapping used in this work can cut the readout time from minutes to seconds, and using a pulsed laser that can deliver enough heat to desorb water molecules before the thermal energy diffuses out of the focus spot would increase both the writing speed and the spatial resolution.

3. Conclusion

In summary, we achieved the atomic-thin erasable and rewritable information recorded on a MoS$_2$ monolayer under ambient conditions by modulating and imaging the PL of a MoS$_2$ monolayer with surface water reversible adsorption/desorption. The messages encoded in this way can be at least under triple protections: information is encrypted, and the writing appearance is invisible; the designated MoS$_2$ triangle is camouflaged among a jumble of MoS$_2$ triangles; they can be easily and immediately erased by breath or even saliva. The miniaturization of the equipment needed for the writing/readout processes is feasible and their operations can
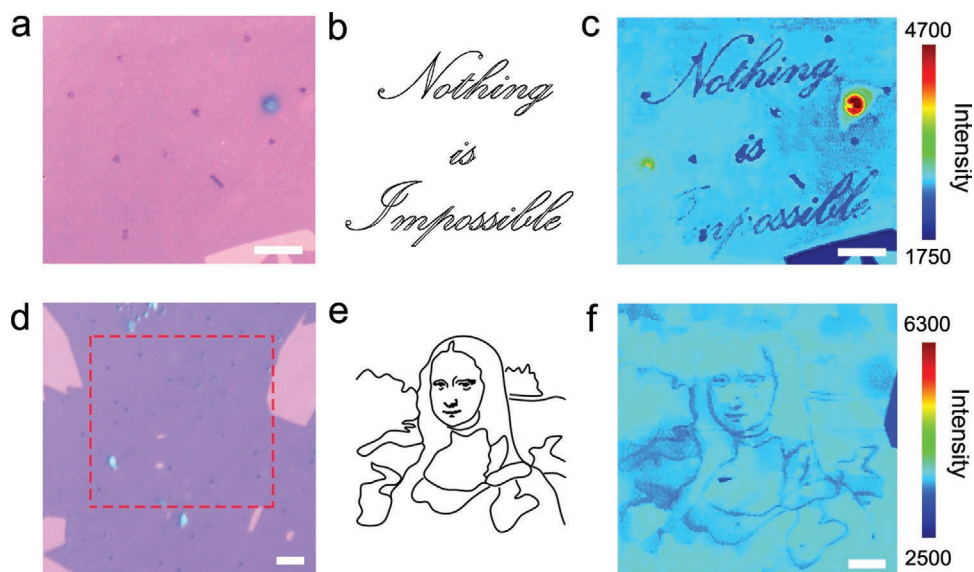

Figure 4. a) Optical image of one MoS$_2$ continuous film monolayer. b) A figure of the phrase "Nothing is Impossible" used as a pattern. c) The PL image corresponding to panel (a) that has been written with the phrase by laser. d) Optical image of another monolayered MoS$_2$ continuous film. The red rectangle denotes the area being mapped. e) A sketch of the famous painting Mona Lisa used as a pattern. f) The PL image corresponding to panel (d) showing the Mona Lisa painting created by laser writing. Scale bars are all 10 µm.

**ADVANCED
SCIENCE NEWS**

www.advancedsciencenews.com

**ADVANCED
MATERIALS
TECHNOLOGIES**

www.advmattechnol.de

be foolproof. These are desirable and promising features for many applications, e.g., steganography, anticounterfeiting, sensors, and transient information storage.

4. Experimental Section

Growth of Monolayer MoS₂: Monolayer MoS_2 was grown on clean 285 nm thick SiO_2/Si wafers in a two-temperature-zone furnace via chemical vapor deposition method. MoO_3 powder (Alfa Aesar, 99.999%, 0.01 g) and sulfur powder (Alfa Aesar, 99.999%, 0.3 g) were used as solid sources. The crucible containing MoO_3 powder was placed 30 cm downstream of the sulfur boat. The SiO_2/Si substrate was positioned facing down at the location of 3 cm downstream from the MoO_3 boat. During growth, 300 sccm Ar gas was used as the carrier gas. After purging Ar gas for 20 min, the temperature for MoO_3 and sulfur powders was raised to 650 and 180 °C, respectively. Then, the monolayer MoS_2 was obtained after ≈7 min of growth.

Laser Writing and Erasing: A home-built laser system was used to process the laser writing operation. The optical setup is illustrated in Figure S2 in the Supporting Information, consisting of a microscopic system and a galvanometric scanning system. A continuous-wave solid-state laser diode (532 nm) was equipped as the laser writing source. A 60× objective lens was used to focus the laser spot into around 2.0 µm. The laser writing path according to the chosen pattern was designed by the software Autodesk (Autodesk Fusion 360). All laser writing processes were performed by using ≈8 mW laser power at room temperature in ambient air. In particular, the laser spot should be accurately focused on the surface of the monolayer MoS_2 to guarantee that the message can be effectively read and erased. The smallest width of lines that could be successfully written and read out was around 0.34 µm. With further optimization, it was expected to be improved by about one order of magnitude. The time to write a message was determined by the carving speed (0.001 s per point in our experiment), and the grid size (distance between points). The messages could be maintained at 30% RH for at least one week. The erasing process was carried out by another humidification treatment in a container connected to a humidifier and a hygrometer to monitor and adjust the humidity in real time.

PL/Raman and AFM Measurements: In this work, a confocal Raman microscopic system (HORIBA, XploRA Plus) equipped with a 532 nm laser and a 100× objective lens was used to obtain PL mappings. The focused laser spot size on the sample was about 0.6 µm. 600 gr mm⁻¹ gratings, 100 µm slit, and 300 µm hole were adapted. The mapping step size was 0.3 µm with swift-on mode, and the integration time on each point was 0.04 s. All measurements were performed by using ≈0.5 mW laser power at room temperature in ambient air. For the single point PL/Raman spectra, the home-built PL/Raman microspectroscopy with a 532 nm laser source and 50× long-working-distance objective lens (0.7 NA) was used, which provided a spot size of ≈2.5 µm. Typical excitation power was 5 mW, and the integration time was 10 s. 600 gr mm⁻¹ grating and 300 µm slit was used to obtain PL spectra, and 1800 gr mm⁻¹ grating and 50 µm slit was used to acquire Raman spectra. Thickness variations of the samples were conducted with the tapping mode by using a commercial AFM (Bruker Dimension Icon with Nanoscope V controller).

Device Fabrication and Testing: To fabricate the FET device, polymethyl methacrylate (PMMA, Microchem, 495 K, A6) was first spin-coated onto the sample as the mask. Auto CAD was adapted to design an area, in order to remove the undesired triangle domains within a 200×200 µm region around the target MoS_2 single domain. This designed area was then exposed by conducting high-resolution electron beam lithography (EBL). Through a precise oxygen plasma etching process, the exposed areas were etched, followed by a subsequent rinse with acetone to remove the top PMMA layer. Next, a second lithography was performed to create the source and drain electrode patterns. Cr/Au (5 nm/45 nm) electrodes were thermally evaporated onto the substrate, and then acetone was used to remove the PMMA mask. Finally, the device was annealed in vacuum at 200 °C for 3 h to eliminate PMMA residuals and any moisture. The electrical characterizations of the MoS_2 FET device were carried out in ambient air on a probe station using a Keithley 4200 SCS as the parameter analyzer.

Supporting Information

Supporting Information is available from the Wiley Online Library or from the author.

Conflict of Interest

The authors declare no conflict of interest.

Data Availability Statement

Research data are not shared.

[1] United States District Court for the District of Columbia, The James Madison Project v. National Archives & Records Administration, CA98-2737, March **2002**, https://sgp.fas.org/jud/ink-030502.pdf.

[2] C. T. Clelland, V. Risca, C. Bancroft, *Nature* **1999**, *399*, 533.

[3] N. Goldman, P. Bertone, S. Chen, C. Dessimoz, E. M. LeProust, B. Sipos, E. Birney, *Nature* **2013**, *494*, 77.

[4] M. Cavallini, F. Biscarini, S. Léon, F. Zerbetto, G. Bottari, D. A. Leigh, *Science* **2003**, *299*, 531.

[5] K. Jiang, I. A. Baburin, P. Han, C.-Q. Yang, X.-B. Fu, Y.-F. Yao, J.-T. Li, E. Cánovas, G. Seifert, J.-S. Chen, M. Bonn, X.-L. Feng, X.-D. Zhuang, *Adv. Funct. Mater.* **2020**, *30*, 1908243.

[6] T.-L. Yu, Y.-F. Wang, K.-Y. Jiang, G.-Q. Zhai, C.-C. Ke, J.-C. Zhang, J.-T. Li, D. Tranca, E. Kymakis, X.-D. Zhuang, *Chem. - Eur. J.* **2021**, *27*, 6340.

[7] Z.-Y. Chen, Y.-H. Chen, Y.-Z. Zhao, F. Qiu, K.-Y. Jiang, S.-H. Huang, C.-C. Ke, J.-H. Zhu, D. Tranca, X.-D. Zhuang, *Langmuir* **2021**, *37*, 2523.

[8] R. Bennewitz, J. N. Crain, A. Kirakosian, J.-L. Lin, J. L. McChesney, D. Y. Petrovykh, F. J. Himpsel, *Nanotechnology* **2002**, *13*, 499.

[9] F. E. Kalff, M. P. Rebergen, E. Fahrenfort, J. Girovsky, R. Toskovic, J. L. Lado, J. Fernández-Rossier, A. F. Otte, *Nat. Nanotechnol.* **2016**, *11*, 926.

[10] V. Garcia, M. Bibes, *Nat. Commun.* **2014**, *5*, 4289.

[11] J. Repp, G. Meyer, F. E. Olsson, M. Persson, *Science* **2004**, *305*, 493.

[12] F. D. Natterer, K. Yang, W. Paul, P. Willke, T. Choi, T. Greber, A. J. Heinrich, C. P. Lutz, *Nature* **2017**, *543*, 226.

[13] S. Loth, S. Baumann, C. P. Lutz, D. M. Eigler, A. J. Heinrich, *Science* **2012**, *335*, 196.

[14] B. Kiraly, A. N. Rudenko, W. M. J. van Weerdenburg, D. Wegner, M. I. Katsnelson, A. A. Khajetoorians, *Nat. Commun.* **2018**, *9*, 3904.

[15] K. Salaita, Y. Wang, C. A. Mirkin, *Nat. Nanotechnol.* **2007**, *2*, 145.

[16] D. S. Ginger, H. Zhang, C. A. Mirkin, *Angew. Chem., Int. Ed.* **2004**, *43*, 30.

[17] A. Ivanisevic, C. A. Mirkin, *J. Am. Chem. Soc.* **2001**, *123*, 7887.

[18] G. Liu, M. Hirtz, H. Fuchs, Z. Zheng, *Small* **2019**, *15*, 1900564.

[19] D. M. Eigler, E. K. Schweizer, *Nature* **1990**, *344*, 524.

[20] J. A. Stroscio, D. M. Eigler, *Science* **1991**, *254*, 1319.

[21] S. Mouri, Y. Miyauchi, K. Matsuda, *Nano Lett.* **2013**, *13*, 5944.

[22] D.-H. Lien, S. Z. Uddin, M. Yeh, M. Amani, H. Kim, J. W. Ager, E. Yablonovitch, A. Javey, *Science* **2019**, *364*, 468.

[23] H. Nan, Z. Wang, W. Wang, Z. Liang, Y. Lu, Q. Chen, D. He, P. Tan, F. Miao, X. Wang, J. Wang, Z. Ni, *ACS Nano* **2014**, *8*, 5738.

[24] C. Tan, X. Cao, X.-J. Wu, Q. He, J. Yang, X. Zhang, J. Chen, W. Zhao, S. Han, G.-H. Nam, M. Sindoro, H. Zhang, *Chem. Rev.* **2017**, *117*, 6225.

[25] Q. Yue, Z. Shao, S. Chang, J. Li, *Nanoscale Res. Lett.* **2013**, *8*, 425.

[26] A. Schumacher, L. Scandella, N. Kruse, R. Prins, *Surf. Sci.* **1993**, *289*, L595.

[27] E. Mieda, R. Azumi, S. Shimada, M. Tanaka, T. Shimizu, A. Ando, *Jpn. J. Appl. Phys.* **2015**, *54*, 08LB07.